CHEMISTRY
AN ASIAN JOURNAL

DOI: 10.1002/asia.200700410

Synthesis and Characterization of Silica@Copper Core–Shell Nanoparticles: Application for Conjugate Addition Reactions

B. Sreedhar,*[a] P. Radhika,[a] B. Neelima,[a] and Neha Hebalkar[b]

Abstract: Silica@copper (SiO_2@Cu) core–shell nanoparticles were synthesized and well characterized by XRD, TEM, AFM, XPS, UV/Vis, TGA–MS, and ICP–AES techniques. The synthesized SiO_2@Cu core–shell nanoparticles were employed as catalysts for the conjugate addition of amines to α,β-unsaturated compounds in water to obtain β-amino carbonyl compounds in excellent yields in shorter reaction times. Furthermore, the catalyst works well for hetero-Michael addition reactions of heteroatom nucleophiles such as thiols to α,β-unsaturated compounds. As the reaction is performed in water, it allows for easy recycling of the catalyst with consistent activity.

Keywords: copper · Michael addition · nanostructures · reusability · water

Introduction

In recent years, research has been directed towards the synthesis and application of metal nanoparticles owing to their unique properties compared to bulk metals.[1] Among the different metal particles, copper nanoparticles have received considerable attention because of their unusual properties and potential applications in diverse fields.[2] The various synthetic procedures for their synthesis include microemulsion,[3] reverse micelles,[4] reduction of aqueous copper salts,[5] UV-light irradiation,[6] vapor deposition,[7] and impregnation methods.[8] In recent years, particular interest has been focused on surface modification of the nanostructures to form core–shell structures, conventionally denoted as core@shell. The surface characteristics of the colloidal particles can be tailored with suitable shell materials, and the properties of core–shell structures can be modified by control over the radius ratio of the core and shell.[9] Core–shell particles are of great interest owing to their potential applications in diverse fields including drug delivery, photonics, sensors, catalysis, etc. Dominguez-Quintero et al. synthesized nanostructured palladium materials supported on silica for the catalytic hydrogenation of benzene, 2-hexanone, and cyclohexanone.[10a] Hori et al. reported the catalytic performance of silica-coated Pt metal particles for the competitive oxidation of methane and other higher hydrocarbons with gaseous oxygen.[10b] Corma et al. reported Pd nanoparticles embedded in a porous sponge-like silica as a suitable catalyst for the Suzuki–Miyaura coupling of electron-rich aryl bromides.[10c] Silica nanoparticles as a core are well studied because of their easy synthesis and the accurate control over their size and size distribution.

Conjugate addition or Michael addition of a wide range of heteroatom nucleophiles to α,β-unsaturated compounds is an important new bond-forming strategy and has attracted special attention in synthetic organic chemistry. The versatility of the conjugate additions is due to the usage of a large variety of Michael donors and acceptors. In particular, the conjugate addition of nitrogen nucleophiles to α,β-enones (aza-Michael reaction) is the most common method for carbon–nitrogen bond formation. Heterocyclic compounds containing the β-amino carbonyl functionality are essential intermediates in the fine chemicals and pharmaceutical industry.[11] The classical Mannich-type reactions are certainly very powerful but need quite severe reaction conditions and are rather sluggish, thereby causing limitations in their use in practice.[12]. However, these reactions require basic[13] or acidic catalysts,[14] which seem to be detrimental to the desired synthesis. To overcome some of the disadvantages, several Lewis acid catalysts have been reported over the past few years.[15] Accordingly, several heterogeneous catalysts

[a] Dr. B. Sreedhar, P. Radhika, Dr. B. Neelima
Inorganic and Physical Chemistry Division
Indian Institute of Chemical Technology
Hyderabad 500007 (India)
Fax: (+91) 40-271-60921
E-mail: sreedharb@iict.res.in

[b] Dr. N. Hebalkar
International Advanced Research Centre for
Powder Metallurgy and New Materials
Balapur PO
Hyderabad 500005 (India)

such as clays,[16] hydrotalcites,[17] KF/Al_2O_3,[18] $CeCl_3{\cdot}7H_2O$/NaI supported on silica and alumina,[19] ionic liquids,[20] and copper nanoparticles[21] have been developed. Furthermore, solvent-free[22] and catalyst-free[23] conjugate addition reactions have also been reported.

As part of our ongoing research on the synthesis, characterization, and applications of silica@metal core–shell nanoparticles,[9d,e] we herein report the synthesis of SiO_2@Cu core–shell nanoparticles (Scheme 1) and the catalytic application for conjugate addition reactions. The synthesized core–shell nanoparticles are well characterized by various techniques and are employed as a recyclable catalyst for the conjugate addition of amines, diamines, and thiols with α,β-unsaturated compounds in water at room temperature to produce the corresponding Michael adducts in excellent yields in shorter reaction times (Scheme 2).

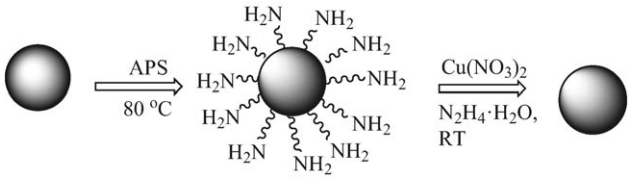

Scheme 1. Synthesis of SiO_2@Cu core–shell nanoparticles

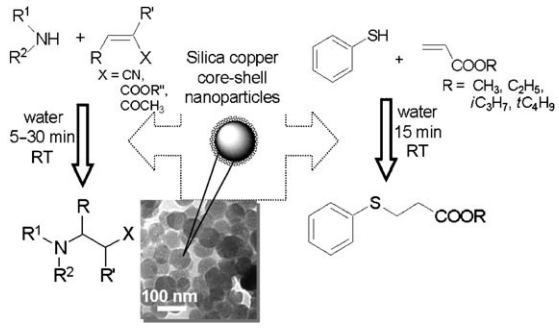

Scheme 2. Conjugate addition of amines and thiophenol to α,β-unsaturated compounds

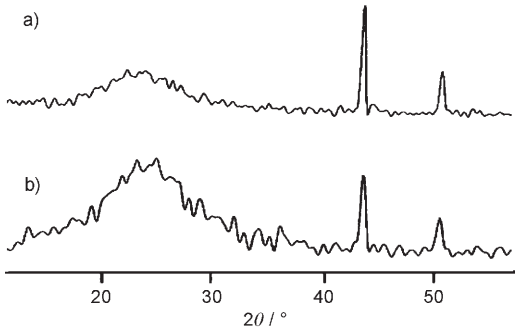

Figure 1. XRD pattern of fresh (a) and used (b) SiO_2@Cu core–shell nanoparticles

Results and Discussion

Characterization of SiO_2@Cu Core–Shell Nanoparticles

SiO_2@Cu core–shell nanoparticles were well characterized by various techniques. The X-ray powder diffraction pattern of the fresh and used catalyst show a signature for Cu^0 and silica as shown in Figure 1. The broad peak at around 23° is due to amorphous silica, which is used as the core. The peaks at 43.2° and 50.6° confirm the presence of Cu^0 in the sample. The XRD pattern of used catalyst also showed characteristic peaks as that of the fresh catalyst, thus suggesting the stability of the catalyst.

TEM studies of both fresh and used SiO_2@Cu core–shell nanoparticles were carried out to understand the shape and size of the particles. Figure 2 shows the transmission electron micrographs for SiO_2@Cu core–shell nanoparticles of diameter 50–60 nm. In the fresh catalyst, the distinction of core and shell was not possible, and they look similar to the core particles with slightly different contrast, as shown in Figure 2a. This may be due to the very thin shell, which was beyond the scope of the used electron microscope. It can also be seen that the fresh as well as the used SiO_2@Cu core–shell nanoparticles do not show any signs of agglomeration. However, the selected area diffraction depicted in the

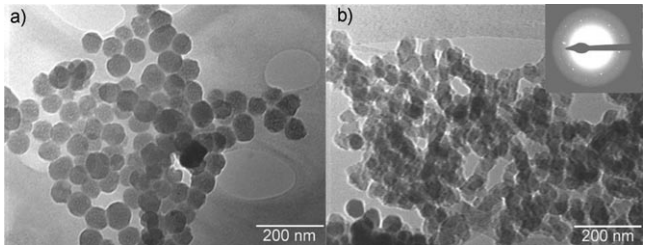

Figure 2. Transmission electron micrographs of fresh (a) and used (b) SiO_2@Cu core–shell nanoparticles.

Abstract in Telugu:

సిలికా పైన కాపర్ (SiO_2@Cu) కోర్-షెల్ నానోకణ ములను సంశ్లేషణ చేసి ఎక్స్ ఆర్ డి (XRD), టి ఇ ఎం (TEM), ఎ యఫ్ ఎం (AFM), ఎక్స్ పి ఎస్ (XPS), యువి-విస్ (UV/Vis), టి జి ఎ-ఎం ఎస్ (TGA-MS) మరియు ఐ సి పి-ఎ ఇ ఒస్ (ICP-AES)వంటి అధునాతన సాంకేతిక పద్ధతులను ఉపయోగించి విశ్లేషించబడినవి. SiO_2@Cu నానోకణ ములను ఉత్ప్రేరకముగా ఉపయోగించి α,β-అసంతృప్త సమ్మేళన ములకు అమీన్‌లతో నీటిలో సంయుగ్మ సంకలన చర్య జరుపబడినది. వాటి ఫలిత ముగా అతి తక్కువ చర్యాస మయము మరియు అధిక మొత్తంలో β-అమైనో కార్బొనైల్ సమ్మేళన ములు ఉత్పత్తికాబడినవి. అదే విధముగా α, β-అసంతృప్త సమ్మేళన ములకు థయోల్ వంటి విజాతీయ పరమాణు న్యూక్లియోఫైల్‌తో విజాతీయ-మైఖేల్ (Hetero-Michael) సంకలనచర్యలు జరపబడినపుడు కూడ SiO_2@Cu నానోకణ ములు ఉత్తమ ఉత్ప్రేరకముగా నిరూపించబడినవి. పైన పేర్కొనబడిన రసాయన చర్యలను నీటిలో జరుపుటవలన ఉత్ప్రేరకమును చర్యాశీలత తీసివేయకుండా సులభ ముగా పునరుత్పత్తి చేయవచ్చును.

inset of Figure 2b shows the diffraction rings for core–shell particles, unlike that of the pure silica particles. This confirms the presence of a thin shell of copper on the silica core particles. Interestingly it is observed that the shape and size of the particles remain unchanged and support the proposal that the morphology of the catalyst remains the same even in the used catalyst. The particle size distribution of SiO_2@Cu core–shell nanoparticles is given in Figure 3 and shows that the highest distribution of the particles is in the range 50–60 nm.

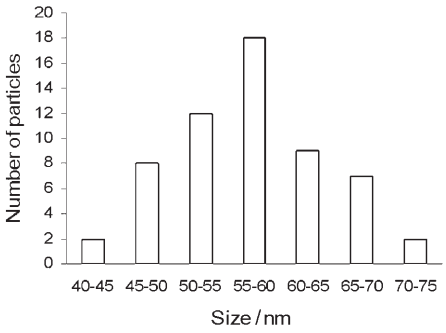

Figure 3. A histogram plot of particle size distribution of SiO_2@Cu core–shell nanoparticles (mean diameter: 57 nm) based on TEM.

AFM analysis (Figure 4) provides three-dimensional structural information of the SiO_2@Cu core–shell nanoparticles. The particle size measurements obtained from the AFM images were the same as those observed from TEM. Figure 4a shows an overview of SiO_2@Cu nanoparticles at a scan size of $1 \times 1\ \mu m^2$ with an average size of about 50 nm, and the majority of the particles are separated from each other, suggesting that the nanoparticles are stabilized against agglomeration. Line scan size analysis further demonstrated that the nanoparticles exhibited a good aspect ratio between height and diameter (Figure 4b).

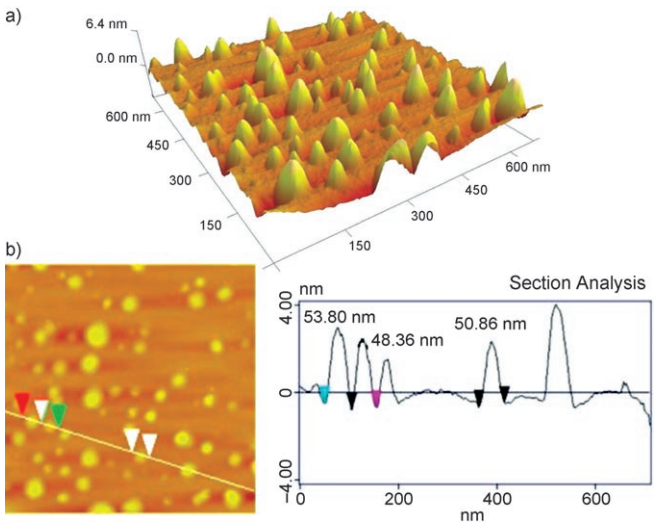

Figure 4. AFM images of fresh catalyst (a) with line scan size analysis (b) of SiO_2@Cu core–shell nanoparticles.

XPS is an important surface-sensitive analytical technique useful for the identification of elements present in SiO_2@Cu core–shell nanoparticles. It also gives stoichiometric information on the constituent elements present in the nanoparticles and the chemical environment around the elements. XPS survey scan of the surfaces of SiO_2@Cu core–shell nanoparticles showed the presence of oxygen (535 eV), silicon (103 eV), and copper (935 eV). High-resolution narrow scans for Cu 2p in the catalyst showed binding energy peaks at 932.4 and 952.3 eV corresponding to $Cu\,2p_{3/2}$ and $Cu\,2p_{1/2}$ photoelectron transitions, respectively, which is characteristic of Cu in the zero-oxidation state (Figure 5a). The used

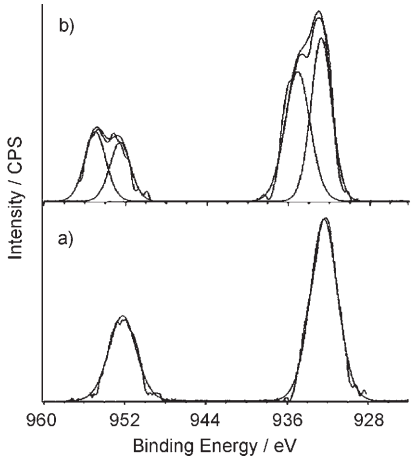

Figure 5. XPS high-resolution narrow scans of fresh (a) and used (b) SiO_2@Cu core–shell nanoparticles. CPS = counts per second

catalyst (Figure 5b), on the other hand, showed two broad peaks at 934 and 952 eV, which are deconvoluted into two peaks each for $Cu\,2p_{3/2}$ at 932.6 and 934.3 eV and $Cu\,2p_{1/2}$ at 952.6 and 954.9 eV. The peaks for $Cu\,2p_{3/2}$ at 934.3 eV and $Cu\,2p_{1/2}$ at 954.9 eV are characteristic of Cu in the +2 oxidation state, from CuO formed during recycling.[24] However, it is interesting to note that partial oxidation of the catalyst does not influence the efficiency of the catalyst, and the catalyst was reused for five cycles with consistent activity.

UV/Vis absorption spectrum of SiO_2@Cu core–shell nanoparticles dispersed in cyclohexane shows a band around 588 nm, which is within the range 550–600 nm reported as the surface plasmon band characteristic of copper nanoparticles (Figure 6). The shifts in the plasmon band depend on the size and shape of the nanoparticles.[25,26] Copper nanoparticles with 30–50 nm diameter show a plasmon band at 579 nm, whereas nanorods with 50–70 nm size show a plasmon band at 586 nm.[27] The observed plasmon band for SiO_2@Cu core–shell nanoparticles is due to the copper nanoparticles deposited over the Si core, which suggests that the effective particle size of the SiO_2@Cu core–shell nanoparticles is within the range 50-60 nm, which is in accord

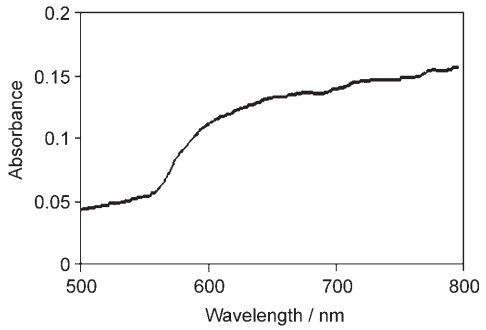

Figure 6. UV/Vis absorption spectrum of SiO_2@Cu core–shell nanoparticles in cyclohexane.

with the mean diameter of 57 nm observed from the TEM studies.

The synthesized SiO_2@Cu core–shell nanoparticles were subjected to TGA–MS to detect the evolved gas fragments, which confirms the presence of the spacer 3-aminopropylsilane on the synthesized catalyst. The thermogravimetric profile of the catalyst in Figure 7 shows a two-step degradation process. As can be seen from the figure, the 3-aminopropylsilane spacer used to anchor copper nitrate on the monodispersed silica nanoparticles degrades in the second degradation step in the temperature range 250–400 °C. The observed TGA–MS evolved gas fragments in this temperature range having *m*/*z* values of 16, 30, 44, and 58, corresponding to NH_2, CH_2NH_2, $(CH_2)_2NH_2$, and $(CH_2)_3NH_2$ fragments, respectively, confirm the presence of the spacer 3-aminopropyl group in the catalyst.

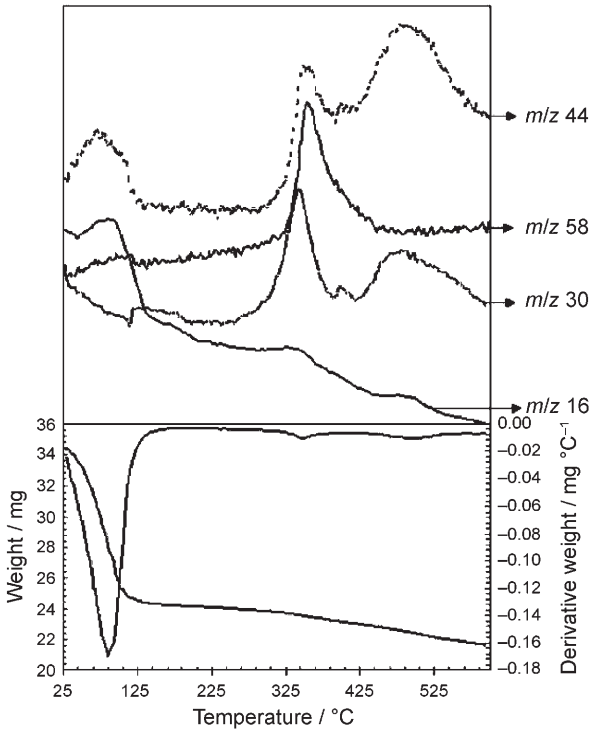

Figure 7. TGA–DTG–MS thermogram profile for SiO_2@Cu core–shell nanoparticles

Catalytic Activity of Silica–Copper SiO_2@Cu Core–Shell Nanoparticles

The synthesized SiO_2@Cu core–shell nanoparticles were employed as catalysts for aza-Michael additions of amines to α,β-unsaturated compounds (Scheme 3). A variety of α,β-

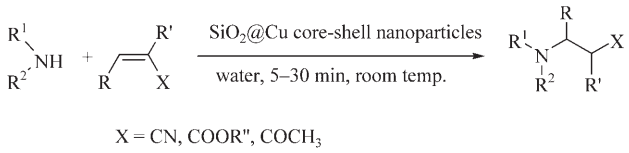

Scheme 3. Aza-Michael addition of amines to α,β-unsaturated compounds.

unsaturated compounds such as methyl acrylate, acrylonitrile, methyl vinyl ketone, cyclohexenone were subjected to reaction with different aliphatic amines in the presence of 1 mol % of SiO_2@Cu core–shell nanoparticles in water at room temperature to give the corresponding β-amino carbonyl compounds in high yields, and the results are summarized in Table 1.

To confirm the critical role of the SiO_2@Cu core–shell nanoparticles, control reactions were conducted under identical conditions using morpholine and acrylonitrile as model substrates. The reaction using monodispersed silica nanoparticles and amino-functionalized silica particles gave the product in low yields (ca. 30 %) whereas the reaction using SiO_2@Cu core–shell nanoparticles as catalyst gave the product in excellent yields in very short reaction times. The presence of copper enhanced the yield of the product and also reduced the reaction time, suggesting the superior activity of SiO_2@Cu core–shell nanoparticles. Further, to study the scope and practical applicability of the catalyst, the reaction was carried out on a larger scale (20 mmol) and the reaction was complete in 15 min to afford the desired product in 95 % yield (Table 1, entry 1). After completion of the reaction, the catalyst was quantitatively recovered by centrifugation and reused for five consecutive cycles with consistent activity (Table 1, entry 1). The copper content in the catalyst after the fifth cycle, as determined by ICP–AES analysis. was found to be 2.07 %.

Simple and long-chain acrylates were equally reactive with morpholine. Branched acrylates such as isobutyl and *tert*-butyl acrylate required slightly longer reaction times than *n*-butyl acrylate (Table 1, entries 3–5). The reaction of morpholine with α,β-substituted Michael acceptors like methyl methacrylate and cyclic α,β-unsaturated ketones such as cyclohexenone afforded the corresponding 1,4-adducts in moderate yield, which may be due to the steric effects of the side chain of the acceptors (Table 1, entries 6-8). Different amines such as piperidine and sterically hindered amines like dibenzyl amine, diisopropyl amine, and dibutyl amine as substrates of this reaction gave the desired products in high yields in shorter reaction times (Table 1, entries 9–14). When primary amines and piperazine were al-

CHEMISTRY
AN ASIAN JOURNAL

Table 1. Aza-Michael reaction of amines with α,β-unsaturated compounds using SiO_2@Cu core–shell nanoparticles.[a]

Entry	Amine	Acceptor	*t* [min]	Product	Yield [%][b]
1			4	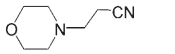	98 95[c] 95[d]
2			5	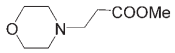	90
3			5	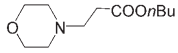	90
4			15	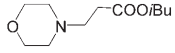	90
5		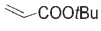	15	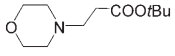	88
6			30	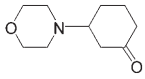	70
7		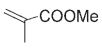	20	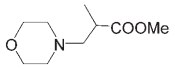	80
8			15	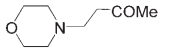	80
9			1	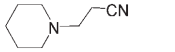	95
10			5	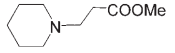	90
11			5	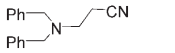	90
12			6	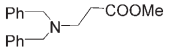	88
13			5	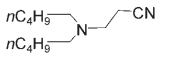	90
14			5		90
15			5		90
16			10		95[c]
17			10		90[e]
18			9		90[e]
19			9		90[e]
20			7		88[e]
21			20		88
22			25		88
23			30		90

[a] Reaction conditions as exemplified in the Experimental Section. [b] Yield of isolated product. [c] Yield of isolated product after fifth cycle. [d] Reaction on 20-mmol scale. [e] Two equivalents of acceptor used.

lowed to react with an excess of Michael acceptor, bis-addition products were observed (Table 1, entries 16–20). Substituted piperazines on reaction with acrylonitrile gave the products in high yields (Table 1, entries 21 and 22). Similarly, imidazole on reaction with acrylonitrile afforded the corresponding N-substituted imidazole in excellent yield (Table 1, entry 23).

To explore the feasibility of the catalyst for aza-Michael addition of diamines, we studied the tandem bis-aza-Michael addition of ethylene diamine and acrylonitrile by varying their relative molar ratios (Scheme 4). One equivalent of diamine with two equivalents of acrylonitrile gave the disubstituted diamine in 70% yield, whereas four equivalents of acrylonitrile gave tetrasubstituted diamine product in 75% yield.

Encouraged by the versatility and effectiveness of the catalyst for the aza-Michael reactions, we attempted to study the hetero-Michael addition of α,β-unsaturated esters with

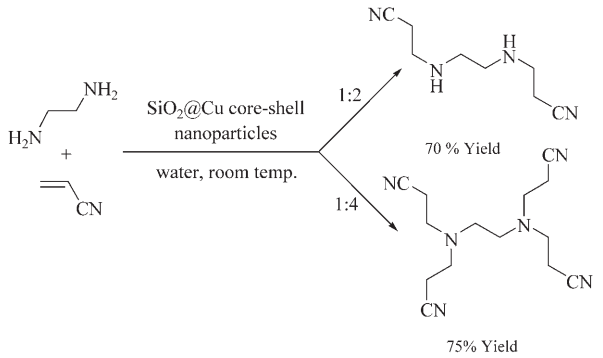

Scheme 4. Tandem bis-aza-Michael addition of ethylene diamine and acrylonitrile

thiols (Scheme 5). At room temperature, thiophenol was introduced at the β-position of different acrylates with ease to afford the corresponding Michael adducts in good yields

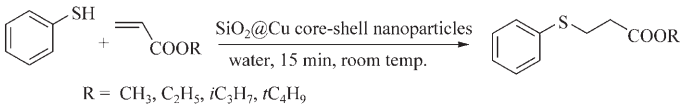

Scheme 5. Hetero-Michael addition of thiols to α,β-unsaturated compounds

(Table 2). Simple and branched acrylates were equally effective for the reaction with thiophenol, and the reactions were completed in shorter reaction times. Furthermore, the catalyst was reused for five cycles with consistent activity (Table 2, entry 1).

Table 2. Michael reaction of thiophenol with α,β-unsaturated esters using SiO_2@Cu core–shell nanoparticles.[a]

Entry	Acceptor	Product	Yield [%][b]
1	COOMe	S COOMe	95 90[c]
2	COOEt	S COOEt	92
3	COO*n*Bu	S COO*n*Bu	90
4	COO*i*Bu	S COO*i*Bu	85
5	COO*t*Bu	S COO*t*Bu	88

[a] Reaction conditions as exemplified in the Experimental Section. [b] Yield of isolated product. [c] Yield of isolated product after fifth cycle.

Conclusions

SiO_2@Cu core–shell nanoparticles were synthesized, well characterized, and employed as catalyst for the conjugate addition of amines, diamines, and thiols to α,β-unsaturated compounds to afford the corresponding products in excellent yields in shorter reaction times. It is remarkable that the reaction in water makes the procedure quite simple, environmentally benign, and allows easy recyclability of the catalyst. Furthermore, catalytic applications of SiO_2@Cu core–shell nanoparticles for addition reactions with complex structures of biological significance are currently under investigation.

Experimental Section

General

Powder X-ray diffraction (XRD) data of the samples were obtained using a Siemens D 5000 X-ray diffractometer with Bragg–Brentano geometry having $Cu_{K\alpha}$ radiation (40 kV, 30 mA), fixed slits, and a graphite secondary monochromator. The samples were scanned for 2θ values ranging from 2° to 65°. Nanosize and morphology of the Si@Cu core–shell nanoparticles were observed with a Philips TECNAI-FE12 transmission electron microscope (120 kV). The particles were dispersed in methanol and a drop of it was placed on a formvar-coated copper grid followed by air drying. Atomic force microscopy (AFM) was employed to characterize the morphology of the nanoparticles using a Digital Nanoscope IV (Veeco Instruments, Santa Barbara, CA).The microscope was vibration damped. Commercial phosphorous (n-)doped silica tips on an I-tape cantilever with a length of 115–135 μm and resonance frequency of about 260 kHz were used. Tapping-mode AFM allows the imaging of the soft samples at high resolution without damaging the sample. X-ray photoelectron spectroscopy (XPS) measurements were obtained on a KRATOS-AXIS 165 instrument equipped with dual aluminum–magnesium anodes using $Mg_{K\alpha}$ radiation. The X-ray power supply was run at 15 kV and 5 mA. The pressure of the analysis chamber during the scan was 10^{-9} Torr. The peak positions were based on calibration with respect to the C1s peak at 284.6 eV. The obtained XPS spectra were fitted using a nonlinear square method with the convolution of Lorentzian and Gaussian functions after the polynomial background subtraction from the raw data. UV/Vis spectra were recorded on a GBC Cintra 10e ultraviolet/visible spectrometer with diffused reflectance spectra (DRS) accessory in the wavelength range 200–800 nm at room temperature with a scan speed of 200 nm and slit width 1.2 nm. Thermogravimetric (TG), differential thermal analysis (DTA), and the mass of the gas evolved during the thermal decomposition of the catalyst were studied on a TGA/SDTA Mettler Toledo 851^e system coupled to a MS Balzers GSD 300 T, using open alumina crucibles containing samples weighing about 8–10 mg with a linear heating rate of 10 °C min^{-1}. Nitrogen was used as purge gas for all these measurements.

Tetraethylorthosilicate (TEOS), 3-aminopropyl trimethoxysilane (APS), $Cu(NO_3)_2.3H_2O$, methyl acrylate, acrylonitrile, methyl vinyl ketone, and amines were purchased from Aldrich or Fluka and used without further purification. ACME silica gel (100–200 mesh) was used for column chromatography, and thin-layer chromatography was performed on Merck-precoated silica gel 60-F254 plates. All the other chemicals and solvents were obtained from commercial sources and purified using standard methods.

Synthesis of Functionalized Monodispersed Silica Core Nanoparticles

Monodispersed silica core nanoparticles were synthesized according to the procedure reported by Stöber et al.[28] Tetraethylorthosilicate (TEOS), ethanol, water, and ammonium hydroxide were mixed in a 1:75:31:4 molar ratio and stirred for three hours. The silica particles were collected by centrifugation and washed three times with water. All the particles were redispersed in 150 mL water, and 10^{-3} mol of 3-aminopropyl trimethoxysilane (APS) was added to it. The solution was stirred at 80 °C for one hour and allowed to cool. The surface-modified silica nanoparticles were collected by centrifugation, washed three times with water, and dried at room temperature in air.

Synthesis of Silica–Copper Core–Shell Nanoparticles

Surface modified silica particles (100 mg) were re-dispersed in water (200 mL) by stirring for 30 min and sonicated for 15 min. Copper nitrate (0.002 M) followed by hydrazine hydrate (6 mL) were added and stirred for 3 h. Finally, the particles were washed with water and dried under vacuum. The copper content in the catalyst was found to be 2.08% by ICP–AES analysis.

General Procedure for the Aza-Michael Reaction of Amines with α,β-Unsaturated Compounds

The mixture of catalyst (0.005 g, 1.08 mol%), amine (1 mmol), and α,β-unsaturated compound (1 mmol) in water (3 mL) was stirred at room temperature for the appropriate time (Table 1). After completion of the reaction, as indicated by TLC, the product was extracted with ethyl acetate (3×10 mL). The combined organic extracts were concentrated in vacuum, and the resulting product was purified by column chromatography on silica gel with ethyl acetate and *n*-hexane (2:8) as eluent to afford the pure β-amino adduct. Similarly, thiols were subjected to the reaction under identical conditions (Table 2). The aqueous layer containing the catalyst was preserved for the next run. The products were characterized by comparison of their NMR and mass spectra with those of authentic samples.[15,19,21a,22b]

Acknowledgements

P.R. thanks the Director, Indian Institute of Chemical Technology (IICT), Hyderabad, India for financial support under the project CNP-0222–18. B.N. thanks the Council of Scientific and Industrial Research (CSIR), New Delhi, India, for the award of Senior Research Fellowship (SRF).

[1] a) J. H. Fendler, *Chem. Rev.* **1987**, *87*, 877–899; b) M. Brust, C. J. Kiely, *Colloids Surf. A* **2002**, *202*, 175–186; c) A. C. Templeton, W. P. Wuelfing, R. W. Murray, *Acc. Chem. Res.* **2000**, *33*, 27- 36; d) L. N. Lewis, *Chem. Rev.* **1993**, *93*, 2693–2730; e) J. P. Novak, L. C. Brousseau III, F. W. Vance, R. C. Johnson, B. I. Lemon, J. T. Hupp, D. L. Feldheim, *J. Am. Chem. Soc.* **2000**, *122*, 12029–12030.

[2] a) L. Lu, M. L. Sui, K. Lu, *Science* **2000**, *287*, 1463–1467; b) J. A. Eastman, S. U. S. Choi, S. Li, W. Yu, L. J. Thompson, *Appl. Phys. Lett.* **2001**, *78*, 718–720; c) G. Larsen, S. Noriega, *Appl. Catal. A.* **2004**, *278*, 73–81.

[3] L. M. Qi, J. M. Ma, J. L. Shen, *J. Colloid Interface Sci.* **1997**,*186*, 498–500.

[4] I. Lisiecki, M. Biorling, L. Motte, B. Ninham, M. P. Pileni, *Langmuir* **1995**, *11* 2385–2392.

[5] X. Ren, D. Chen, F. Tang, *J. Phys. Chem. B* **2005**, *109*, 15803–15807.

[6] S. Kapoor, D. K. Palit, T. Mukherjee, *Chem. Phys. Lett.* **2002**, *355*, 383–387.

[7] J. Wang, H. Huang, S. V. Kesapragada, D. Gall, *Nano Lett.* **2005**, *5*, 2505–2508.

[8] I. O. Ali, *Mater. Sci. Eng. A* **2007**, *459*, 294–302.

[9] a) S. J. Oldenberg, R. D. Averitt, S. L. Westcott, N. J. Halas, *Chem. Phys. Lett.* **1998**, *288*, 243–247; b) V. V. Hardikar and E. Matijevic, *J. Colloid Interface Sci.* **2000**, *221*, 133–136; c) G. Zhou, M. Lu, Z. Yang, *Langmuir* **2006**, *22*, 5900–5903; d) N. Hebalkar, P. Radhika, B. Sreedhar, M. L. Kantam, *J. Nanosci. Nanotechnol.* **2007**, *7*, 3662–3669; e) B. Sreedhar, P. Radhika, B. Neelima, N. Hebalkar, *J. Mol. Catal. A* **2007**, *272*, 159–163.

[10] a) O. Dominguez-Quintero, S. Martínez, Y. Henríquez, L D′Ornelas, H. Krentzien, J. Osuna, *J. Mol. Catal. A* **2003**, 197, 185–191; b) K. Hori, H. Matsune, S. Takenaka, M. Kishida, *Sci. Technol. Adv. Mater.* **2006**, 7, 678–684; c) G. Budroni, A. Corma, H. García, A. Primo, *J. Catal.* **2007**, 251, 345–353.

[11] a) G. Bartoli, C. Cimarelli, E. Marcantoni, G. Palmieri, M. Petrini, *J. Org. Chem.* **1994**, *59*, 5328–5335; b) Y. Hayashi, J. J. Rode, E. J. Corey, *J. Am. Chem. Soc.* **1996**, *118*, 5502–5503; c) P. Traxler, U. Trinks, E. Buchdunger, H. Mett, T. Meyer, M. Muller, U. Regenass, J. Rosel, N. Lydon, *J. Med. Chem.* **1995**, *38*, 2441–2448; d) S. Fustero, B. Pina, E. Salavert, A. Navarro, M. C. Ramirez de Arellano, A. S. Fuentes, *J. Org. Chem.* **2002**, *67*, 4667–4679; e) L.- W. Xu, C-. G. Xia, X.- X. Hu, *Chem. Commun.* **2003**, 2570–2571.

[12] M. Arend, B. Westermann, N. Risch, *Angew. Chem.* **1998**, *110*, 1096–1122; *Angew. Chem. Int. Ed.* **1998**, *37*, 1044–1070.

[13] a) S. D. Bull, S. G. Davies, S. D.- Ballester, G. Fenton, P. M. Kelly, A. D. Smith, *Synlett* **2000**, 1257–1260; b) S. G. Davies, T. D. Mc Carthy, *Synlett* **1995**, 700–702.

[14] a) J. C. Adrian, M. L. Snapper, *J. Org. Chem.* **2003**, *68*, 2143–2150; b) N. B. Ambhaikar, J. P. Shyger, D. C. Liotta, *J. Am. Chem. Soc.* **2003**, *125*, 3690- 3691.

[15] a) N. Srivastava, B. K. Banik, *J. Org. Chem.* **2003**, *68*, 2109–9052; b) N. Azizi, M. R. Saidi, *Tetrahedron* **2004**, *60*, 383–387; c) C. E. Yeom, M. J. Kim, B. M. Kim, *Tetrahedron* **2007**, *63*, 904–909.

[16] N. S. Shaikh, V. H. Despande, A. V. Bedekar, *Tetrahedron* **2001**, *57*, 9045–9048.

[17] M. L. Kantam, B. Neelima, Ch. V. Reddy, *J. Mol. Catal. A* **2005**, *241*, 147–150.

[18] L. Yang, L.-W. Xu, C. G. Xia, *Tetrahedron Lett.* **2005**, *46*, 3279–3282.

[19] a) G. Bartoli, M. Bosco, E. Marcantoni, M. Pertrini, L. Sanbri, E. Torregiani, *J. Org. Chem.* **2001**, *66*, 9052–9055; b) G. Bartoli, M. Bartolacci, A. Giuliani, E. Marcantoni, M. Massaccesi, E. Torregiani, *J. Org. Chem.* **2005**, *70*, 169–174.

[20] J. M. Xu, C. Qian, B. K. Liu, Q. Wu, X. F. Lin, *Tetrahedron* **2007**, *63*, 986–990.

[21] a) A. K. Verma, R. Kumar, P. Chaudhary, A. Saxena, R. Shankar, S. Mozumdar, R. Chandra, *Tetrahedron Lett.* **2005**, *46*, 5229–5232; b) K. R. Reddy, N. S. Kumar, *Synlett* **2006**, 2246–2250.

[22] a) B. C. Ranu, S. S. Dey, A. Hajra, *ARKIVOC* **2002**, *7*, 76–81; b) G. L. Khatik, R. Kumar, A. K. Chakraborti, *Org. Lett.* **2006**, *8*, 2433–2436.

[23] B. C. Ranu, S. Benerjee, *Tetrahedron Lett.* **2007**, *48*, 141–143.

[24] P. Stefanov, N. Minkovski, I. Balchev, I. Avramova, N. Sabotinov, T. Marinova, *Appl. Surf. Sci.* **2006**, *253*, 1046–1050.

[25] A. Henglein, *J. Phys. Chem.* **1993**, *97*, 5457–5471.

[26] I. Lisiecki, M. P. Pileni, *J. Am. Chem. Soc.* **1993**, *115*, 3887–3896.

[27] D. S. Jacob, I. Genish, L. Klein, A. Gedanken, *J. Phys. Chem. B* **2006**, *110*, 17711–17714.

[28] W. Stöber, A. Fink, E. Bohn, *J. Colloid Interface Sci.* **1968**, *26* , 62–69.

Received: December 12, 2007
Published online: May 16, 2008

